Astron. Astrophys. 322, 533–544 (1997)

ASTRONOMY
AND
ASTROPHYSICS

On the progenitors of double neutron star systems

P. Bagot

GRAAL, UPRESA 5024 CNRS/UMII, Université Montpellier II, CC072, F-34095 Montpellier Cedex 05, France (bagot@graal.univ-montp2.fr)

Received 6 November 1996 / Accepted 20 November 1996

Abstract. We discuss models for calculating the late stages of high-mass binary evolution. Our discussion is based on evolutionary calculations for initial binaries composed of a main-sequence star of mass range 8 to 30 $M_\odot$ with a neutron star companion. The evolution of the primary is followed with the grids of Schaller et al. (1992) until the two stars interact, and simple analytic fits for helium and carbon-oxygen stars. For non-conservative mass transfer phases, two physical processes are considered: ejection of the excess overflowing matter in the form of jets from the neutron star and common envelope (CE) evolution. For each model, the code allows us to find the progenitors of the four known double neutron star systems (NS-NS) in the disk of the Galaxy. We show that the observed parameters of PSR 1913+16 and PSR 1534+12 are consistent with one or two stages of mass transfer. In contrast, the wide orbits of PSR 2303+46 and PSR J1518+49 are the most difficult to reproduce since a moderate orbital shrinkage is required through a CE phase. In particular, the likelihood of the formation of PSR J1518+49 appears to be very sensitive to the adopted formalism for CE-evolution.

Key words: stars: close binaries – stars: evolution – stars: mass loss – neutron stars – WR stars

1. Introduction

The excellent agreement of the observed rate of decrease of the orbital period of PSR 1913+16 system with the theoretical rate predicted by general relativity (Taylor & Weisberg 1989) is considered today as evidence, although indirect, for the existence of gravitational waves. Therefore, the merger of a NS-NS binary appears to be not only one of the most promising sources for the planned gravitational wave detectors Ligo/Virgo, but above all the most important one due to the quality of information which could be extracted from a direct detection (cf. Schutz 1986, Chernoff & Finn 1993).

Much uncertainty remains about the merger rate of NS-NS systems. The first observational estimates (Narayan et al. 1991; Phinney 1991) reported a Galactic disk merger rate ν_c of $\sim 10^{-6}$ yr^{-1}. To date, no further close NS-NS systems have been found by the latest sensitive millisecond pulsar surveys. Using these results and a more recent distance model for pulsars, Curran & Lorimer (1995) estimated a merger rate of 10^{-7} yr^{-1}. However, taking account of the beaming factor and of pulsars with low radio luminosity, they suggested a more realistic value of $\nu_c \sim 3.10^{-6}$ yr^{-1}. In addition, Van den Heuvel & Lorimer (1996) revised the lifetimes τ of observed NS-NS systems and arrived at a Galactic merger rate of $\nu_c \sim 8.10^{-6}$ yr^{-1}. Numerical simulations based on evolutionary scenarios in which neutron stars do not acquire a kick velocity at birth (Tutukov & Yungelson 1993) suggest a larger rate, of up to 3.10^{-4} yr^{-1} (see also Clark et al. 1979), which departs from the Bailes' upper limit of 10^{-5} yr^{-1} for the NS-NS birthrate (Bailes 1996). On the other hand, Monte-Carlo simulations performed with a high kick velocity and with a different treatment of mass and angular momentum losses lead to a merger rate of $\nu_c \sim 2.10^{-5}$ yr^{-1} (Portegies Zwart & Spreeuw 1996), more consistent with observational estimates.

The high sensitivity of the formation rate of NS-NS systems to the late stages of evolution is mainly responsible of the uncertainty in theoretical merger rates. Unfortunately, very few observations of binaries that have evolved beyond the high mass X-ray binary (HMXB) phase are available to constrain evolutionary models for massive close binaries. The only known systems are SS 433, a peculiar binary in which a massive evolved donor transfers matter to the X-ray source at a rate much higher than the Eddington limit (Margon 1984), Cyg X-3 a short-period system composed of a WR star and a compact object (Van Kerkwijk et al. 1992) and the four NS-NS systems in the disk of the Galaxy. It is worth noting that the nature of the compact object (NS/BH) is still unknown in SS 433 and in Cyg X-3. The aim of this paper is to rediscuss the physical processes used to describe the late stages of evolution (Sect. 2) and to constrain these models from the observed parameters of NS-NS systems (Sect. 3). In Sect. 4, we shall discuss the particular case of binary pulsars with a wide orbit for which Van den Heuvel et al. (1994) have proposed an alternative model of formation.

2. Pre-supernova binary systems

2.1. Evolutionary models

2.1.1. General frame

Starting from an evolved binary system composed of a massive main-sequence star (of mass M_0) and a neutron star (of mass

m), we assume that close NS-NS systems are formed through the following stages (e.g. see the review of Bhattacharya & Van den Heuvel 1991):
(1). Stellar wind mass loss phase from the massive star. If enough wind material is accreted onto the neutron star, binary systems appear as standard/Be-type HMXBs.
(2). Non-conservative mass transfer phase when the evolved star overflows its Roche lobe. The remaining system consists of a helium star and a recycled neutron star.
(3). Stellar wind mass loss phase from the helium star (if still on the helium main-sequence).
(4). Possible second non-conservative mass transfer phase from the helium star when helium is exhausted in the core, resulting in the formation of a carbon-oxygen (CO) star.
(5). Supernova explosion with a kick velocity imparted to the newly born neutron star.

In standard scenarios, the physical process used to describe the first non-conservative mass transfer phase involves the rapid formation of a CE around the system, leading to the spiral-in of the neutron star into the envelope. In this picture, the efficiency parameter α_{CE} of orbital momentum transfer into the CE and the kick velocity are the two parameters which correspond to the uncertainty in the late stages of evolution. In the following, we shall describe each stage (1)-(4) for the formation of pre-supernova binaries and extend the parameter space to when there is a lack of theoretical ground to justify the adoption of some particular physical processes.

In the Roche model, the combination of gravitational and centrifugal forces allows one to define sets of points of the same potential. In the particular case of synchronous rotation and circular orbit, a critical equipotential surface intersects itself at the inner Lagrange point L_1, defining the two Roche lobes, one surrounding each star. An accurate expression for the Roche lobe radius R_L of the component with mass M was found by Eggleton (1983):

$$r_L \equiv \frac{R_L}{a} = \frac{0.49}{0.6 + q^{2/3}\ln(1+q^{-1/3})} \quad (1)$$

where q is the mass ratio defined as $q = m/M$ and a is the orbital separation.

Evolutionary tracks for the primary are taken from Schaller et al. (1992) with an initial chemical composition X=0.70 and Z=0.02. The grids include stellar wind mass loss in massive stars and core overshooting with α_{ov}=0.20. Following Thorsett et al. (1993), we assume the mass of the neutron star to be m = 1.35 $M_\odot$. Evolutionary paths for binaries are followed as a function of the initial mass M_0 of the main-sequence star and the initial orbital separation a_0. For our purpose, we ignore the time spent by the primary on the main-sequence phase before the formation of the first neutron star. Thus, the massive binary component is assumed to evolve from the ZAMS as a single star as long as the system remains detached, although it may have accreted matter from the progenitor of the neutron star. We shall discuss this point in Sect.4. The first supernova explosion induced a moderate eccentricity into the orbit. As the massive star expands, tidal interaction tends to circularize the orbital motion. Since the eccentricity has only a second-order effect on the tidal evolution of the orbital separation (Zahn 1977), we make the approximation of initially circular binaries.

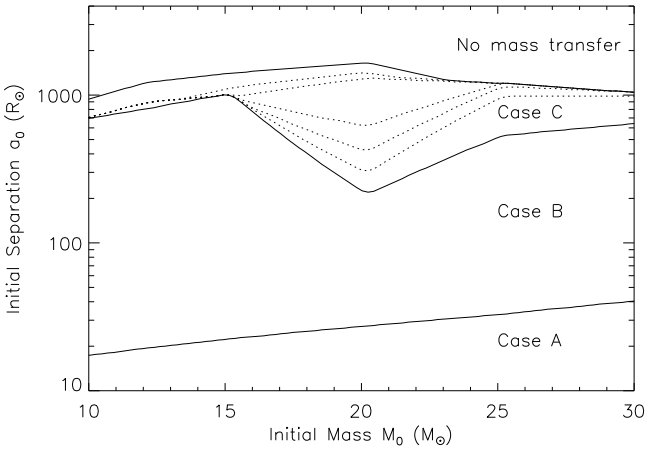

Fig. 1. Evolutionary state of the massive star in a binary with a neutron star companion when the primary first fills its Roche lobe. The 3 solid lines delimit the regions where cases A, B and C of mass transfer occur, respectively core-H exhaustion, He-ignition and more advanced nuclear burning stages of the star. From bottom to top, the dotted lines refer to the central helium content of Yc= 0.95, 0.90, 0.85, 0.80 and 0.0 during the core-He burning phase.

2.1.2. Stellar wind mass loss phase

In most papers, the change in orbital separation during this phase is assumed to occur according to the Jeans' mode (e.g. Tutukov & Yungelson 1993, 1994; Lipunov et al. 1996, Portegies Zwart & Verbunt 1996). In this mode, matter escapes in a spherically symmetric way from the system at a high velocity with the specific angular momentum of the star considered as a point mass. The change in orbital separation then follows from $aM_T = const.$, where M_T is the total mass of the system. This relationship strictly applies to binaries in which the mass-losing star lies deep inside its Roche lobe. For a Roche lobe filling factor $\Phi = R/R_L$ not far from unity (R is the radius of the star), orbital evolution is more likely to be driven by the tidal exchange between rotational and orbital angular momentum. We assume, however, that tidal effects are of secondary importance in view of major uncertainties in the next stage.

2.1.3. Non-conservative mass transfer phase

Due to evolutionary expansion of its envelope, the massive binary component begins to transfer mass to the neutron star through L_1 when it fills its Roche lobe. From grids of stellar models and Eq.(1), we determine the corresponding evolutionary state of the star for each initial set of parameters (M_0, a_0). Fig. 1 depicts the cases A, B and C of mass transfer as defined by Kippenhahn & Weigert (1967).

In binaries of very low mass ratio, mass transfer from the more massive component leads to a rapid decrease of the orbital separation and thereby of the Roche lobe radii[1]. Then, the mass transfer rate depends on the response to mass loss of the donor star (e.g. Hjellming & Webbink 1987). In case A and early case B binaries, the massive star with a radiative envelope out of thermal equilibrium contracts less rapidly than its Roche radius. The mass transfer then proceeds on the thermal time scale . In late case B and case C systems, the deep convective envelope of the evolved star is highly unstable and tends to expand on a dynamical time scale rather than to contract when mass is removed. Therefore, expected mass transfer rates are much larger than in the case of a radiative envelope. In both cases, the accretion rate onto the neutron star is limited by the Eddington rate $\dot{m}_{cr} = 1.5\ 10^{-8}\ \mathrm{M}_{\odot}\ yr^{-1}$ and any further accretion will be prevented by radiation pressure. The excess overflowing matter is expected to form a CE or an extended thick accretion disk around the neutron star. In these two scenarios, binary systems undergo a phase of extensive angular momentum loss.

The important problem of mass accretion onto the neutron star was addressed by Chevalier (1993) and Brown (1995) who found that the Eddington limit does not apply to spherically symmetrical situations with high accretion rates $\dot{M} \geq 10^{-3}$ $\mathrm{M}_{\odot}\ yr^{-1}$. In this regime, neutrino losses allow the neutron star in a dense stellar envelope to accrete a substantial amount of matter with the result of black hole formation. However, Chevalier (1996) showed that for a red supergiant companion, rotation of the gas prevents strong accretion onto the neutron star. In this picture, black hole formation should occur only if the spiral-in continues into the stellar core of the primary. Therefore, we assume that survival binaries after the mass transfer phase are composed of a remnant helium core and a neutron star of negligible accreted mass.

Common envelope evolution

This model is the most frequently used to describe the mass transfer phase in binaries of low mass ratio with a neutron star (e.g. Meurs & Van den Heuvel 1989; Rathnasree 1993; Tutukov & Yungelson 1993, 1994; Pols & Marinus 1994; Portegies Zwart & Verbunt 1996). Once the neutron star is embedded with a differential velocity into the envelope of its companion, orbital evolution is driven by frictional forces, resulting in a spiral-in process. Binaries will survive this phase if energy deposition generated by the large frictional drag allows the ejection of the entire CE carrying with it nearly all of the orbital angular momentum. Then, the final orbital parameters can be calculated by assuming that the loss of orbital energy ΔE_{orb} is used to expel the envelope of binding energy ΔE_{bind} according to $\Delta E_{bind} = \alpha_{CE}\Delta E_{orb}$, where α_{CE} is an efficiency parameter less than or equal to one (Webbink 1984). This prescription leads to the following relation between the original and final orbital separation a_i and a_f (De Kool 1990):

$$\frac{GM_i(M_i - M_f)}{\lambda R_L} = \alpha_{CE}\left(\frac{GM_f m}{2a_f} - \frac{GM_i m}{2a_i}\right) \quad (2)$$

where λ approximated by 0.5 is a factor depending on the mass distribution in the envelope, M_f is the mass of the remnant core. Equation (2) yields:

$$\frac{a_f}{a_i} = \frac{M_f}{M_i}\left(1 + \frac{2}{\lambda r_L \alpha_{CE}}\frac{M_i - M_f}{m}\right)^{-1} \quad (3)$$

For the sake of comparison with previous works, we will take the value of α_{CE} in the range 0.5 to 1.

Jets from the compact star

In non-spherical situations, centrifugal forces keep gas from directly reaching the neutron star surface and matter lost from the massive star may form a supercritical accretion disk around the compact star (Shakura & Sunyaev 1973; Kornilov & Lipunov 1983 a,b; Bhattacharya & Van den Heuvel 1991). Owing to the Eddington limit, the larger part of the transferred matter is expelled from the inner regions of the disk. Following this model, matter is thought to escape from the neutron star in the form of relativistic jets, carrying away its orbital angular momentum.

Van den Heuvel et al. (1980) showed that the occurence of this physical process in SS 433 accounts well for the unusual behaviour of this system. The SS 433 object associated with the X-ray source A1909+04 appears to be an eclipsing binary system with an orbital period of 13.1 days (Crampton et al. 1980). Observational characteristics are usually ascribed to the ejection of collimated jets of matter from a compact object at 0.26c (e.g. see the review of Margon 1984). In most models, the observed periodic rotation of the jet axis is related to the orientation of a thick accretion disk whose plane precesses with a 164 day period. Although the nature of the underlying components are not known exactly, observations suggest that an OB star that has evolved beyond the HMXB phase transfers matter to a compact object through the inner Lagrangean point in a thermal time scale, resulting in a mass transfer rate highly super-Eddington (Cherepashchuck 1981). In addition, Van den Heuvel et al. (1980) and Zealey et al. (1980) estimated a lower limit $\dot{M}_b \geq 10^{-6}\ \mathrm{M}_{\odot}\ yr^{-1}$ for the mass loss rate in the beams.

Thus, observational ground supports a scenario in which orbital evolution is driven by the ejection of matter carrying with it the specific angular momentum of the neutron star as follows. Logarithmic differentiation of total orbital angular momentum $J_{orb} = Mm(Ga/M_T)^{1/2}$ yields:

$$\frac{\dot{a}}{a} = -2\left(\frac{\dot{M}}{M} + \frac{\dot{m}}{m}\right) + \frac{\dot{M}_T}{M_T} + 2\frac{\dot{J}_{orb}}{J_{orb}} \quad (4)$$

The contribution of angular momentum loss due to mass outflow from the inner edge of the disk is given by:

$$\frac{\dot{J}_{orb}}{J_{orb}} = (1 - \beta)\ \frac{M}{mM_T}\ \dot{M} \quad (5)$$

[1] Note that the possible occurence of the Darwin instability (Counselman 1973, Bagot 1996) may already cause the orbit to decay on the tidal time scale at the onset of Roche lobe overflow.

where β is the fraction of matter accreted onto the compact star. Substituting this expression in Eq.(4), we obtain

$$\frac{\dot{a}}{a} = \left(\frac{2}{m} - \frac{2}{M} - \frac{1-\beta}{M_T} \right) \dot{M} \quad (6)$$

Integration of this equation gives the change of the orbital separation:

$$\frac{a_f}{a_i} = \frac{M_T^i}{M_T^f} \left(\frac{M_i}{M_f} \right)^2 \left(\frac{m_i}{m_f} \right)^{2/\beta} \quad (7)$$

where $m_f = m_i + \beta(M_i - M_f)$ and $M_T^f = M_T^i - (1-\beta)(M_i - M_f)$. In the limit $\beta = 0$, the orbital evolution when accretion of matter onto the neutron star is thought to be negligible is given by:

$$\frac{a_f}{a_i} = \frac{M_T^i}{M_T^f} \left(\frac{M_i}{M_f} \right)^2 \exp\left(-2 \, \frac{M_i - M_f}{m} \right) \quad (8)$$

The exponential term in Eq.(8) makes the shrinkage factor a_f/a_i extremely sensitive to the mass ratio. Systems with initial low mass ratio are unlikely to survive this mass transfer phase if all of the hydrogen-rich envelope is ejected through this process. From Eq.(6), the timescale for orbital decay can be approximated by:

$$\frac{a}{\dot{a}} \sim \frac{2q}{1-q} \frac{M}{\dot{M}} \quad (9)$$

Thus, this timescale in binaries containing a neutron star is roughly an order of magnitude shorter than the timescale for mass loss $M/\dot{M}$.

An intermediate model

No hydrodynamical calculation has yet been done which computes the initial stage of the non-conservative mass transfer phase in high-mass binaries containing a compact star. In particular, the spiral-in process in the CE scenario implies that the neutron star is already embedded in the outer layers of the massive companion. The existence of a thick accretion disk with two opposed collimated jets in SS 433 suggests that a substage of fast mass transfer[2] occurs when the massive star begins overflowing its Roche lobe (Lipunov et al. 1996). The further evolution of the system is hard to predict since the thick disk may not remain stable with increasing large mass-transfer rate. It is useful to define a parameter δ which is the fraction of mass lost during this substage of mass transfer: $\delta = \Delta M_{jets}/\Delta M_T$, where ΔM_{jets} corresponds to the amount of matter leaving the system in the form of jets and ΔM_T is the mass of the envelope. Orbital evolution is first computed according to Eq.(8) in which $M_i - M_f = \delta \, \Delta M_T$. When the transferred matter leads to the formation of a common envelope, Eq.(3) is used with $M_i - M_f = (1-\delta) \, \Delta M_T$.

To give an upper limit to the value of δ, we consider a binary with an orbital separation of 500 $R_\odot$. In this system, a 16 $M_\odot$ star has a radius of 300 $R_\odot$ at the onset of mass transfer and a core mass of 5.1 $M_\odot$. According to Eq.(8), the amount of mass loss required to bring the neutron star near the surface of the primary is only of 0.4 $M_\odot$. The distribution of mass for an evolved star with respect to radius favors the rapid formation of a CE as soon as the neutron star encounters the outer layers of its companion. For instance, if one assumes that the ejection of matter still continues in the form of jets, the orbit would decay from the stellar surface to half-radius for an amount of mass ejected of 0.5 $M_\odot$. This is clearly inconsistent with the structure of the 16 $M_\odot$ star since more than approximately 4 $M_\odot$ is located in the outer half of the star (cf. Fig. 1 in Terman et al. 1995). Therefore, we will take $\delta = 0.1$ as a conservative limit for the first mass transfer phase.

2.1.4. Stellar wind mass loss from the helium star

Very close binaries are left after the non-conservative mass transfer phase, consisting of the neutron star and the helium core of the massive star. Vanbeveren & De Greve (1979) found that the mass at the end of a case B mass transfer corresponds to the mass of the convective core during core-H burning when $X_c = X_{atm}$ of the remnant model, where the atmospherical hydrogen abundance X_{atm} is typically 0.25 for Galactic models. Using this criterion, De Loore & Vanbeveren (1994) performed evolutionary computations for massive close binaries, providing a best fit relation between the remnant mass M_{He} and ZAMS mass M_0:

$$M_{He} = -1.069 + 0.317 M_0 + 0.00432 M_0^2 \quad (10)$$

Comparatively few studies have dealt with the third type of binary evolution, case C mass transfer. We extend the previous relationship for the core mass stripped of its hydrogen-rich envelope during the core-He burning stage (CHeB) of the primary. For more advanced nuclear burning stages, we use the prescription of Portegies Zwart & Verbunt (1996):

$$M_{He} = 0.058 \, (1+\gamma) M_0^{1.57} \quad (11)$$

where $\gamma = 0.20$ is a factor taking into account effects of core overshooting (Shore et al. 1994). The outer radius R_{He} of a helium star on the He main-sequence phase is taken from Langer (1989a):

$$\log R_{He} = -0.651 + 0.640 \log M_{He} - 0.0235 (\log M_{He})^2 \quad (12)$$

When the hydrogen-rich envelope has been removed by strong stellar wind mass loss, the further evolution of the helium star remnant is thought to be affected by WR stellar wind mass loss during the CHeB phase. For hydrogenless WR stars, Langer (1989b) introduced mass dependent mass loss rates:

$$\dot{M} = k M^\alpha \quad (13)$$

[2] Note that the timescale for orbital decay (Eq.9) is much longer if binary components are of comparable masses. This suggests the presence of a black hole in SS 433 rather than a neutron star (see also Verbunt & Van den Heuvel 1995).

where α = 2.5, and k = 6 $10^{-8} M_\odot$ yr^{-1} for hydrogenless WN stars and k = $10^{-7} M_\odot$ yr^{-1} for WC/WO stars.

As the surface conditions do not show significant physical difference, helium cores revealed by mass transfer in a binary or by mass loss from a single star, are expected to experience the same stellar wind mass loss. Woosley & al. (1995) have considered the time evolution of mass-losing helium stars with initial masses between 4 and 20 M$_\odot$ according to Eq.(13). An important feature raised from their results (see also Woosley & al. 1993) is the convergence of all helium stars to small final masses in the range 2.26 - 3.55 M$_\odot$. However, they noted that there was weak observational justification in the adopted mass loss rate for helium stars below 5 M$_\odot$.

Recently, Kiriakidis et al. (1993) found that very massive main-sequence stars experience violent pulsational instabilities. These authors reported that the same process also occurs on the helium main-sequence phase (Glatzel et al. 1993). In particular, it was shown that helium stars above $\sim$ 4.5 M$_\odot$ are unstable with respect to radial pulsations. Such instabilities operating on dynamical time-scales are expected to drive a stellar wind with mass-loss rates as observed in WR stars (see also Langer et al. 1994). This lower mass limit above which dynamical unstable modes appear in helium stars suggests a pile up of final masses near this threshold. Furthermore, these instabilities were found to increase with the mass of the helium stars. According to this picture, the power-law index α introduced by Langer can be consistently related to the growing strength of pulsational instability.

In high-mass binaries, mass transfer can lead to initial helium star mass as small as $\sim$ 2.5 M$_\odot$. In order to take into account the effects of pulsational instability, we introduce a lower mass limit M_l above which a helium star experiences stellar wind mass loss. Equation (13) was constructed with the necessary condition $\dot{M}(M \rightarrow 0) \rightarrow 0$. The new necessary condition $\dot{M}(M \rightarrow M_l) \rightarrow 0$ allows us to rewrite the mass-dependent mass loss rate as:

$$\dot{M} = k(M^\alpha - M_l^\alpha) \qquad (14)$$

where k and α have the same values as in Eq.(13) and M_l = 4.5 M$_\odot$. Fig. 2 shows that well-established high mass loss rates for massive helium stars are also provided when incorporating M_l in Eq.(13).

As outlined in Langer (1994), the final outcome of WR models depends mainly on the value of the central helium content Y_c at the beginning of the WR stage. Single massive stars spend a large part of their helium burning lifetime on the red supergiant branch and reach the WR regime at a much smaller Y_c (e.g. $Y_c \leq 0.50$ for a single 40 M$_\odot$ star) than binary stars experiencing a case B mass transfer. Fig. 1 shows that helium cores stripped of their hydrogen-rich envelope during CHeB turn into the WR stage at $Y_c \geq 0.80$. This is due to the fact that the maximal radius of a massive star during CHeB is reached at the early stages of this phase. For these stars and case B primaries, final helium star masses are computed according to Eq.(14) with the approximation of Y_c = 1.00 at the beginning of the WR stage.

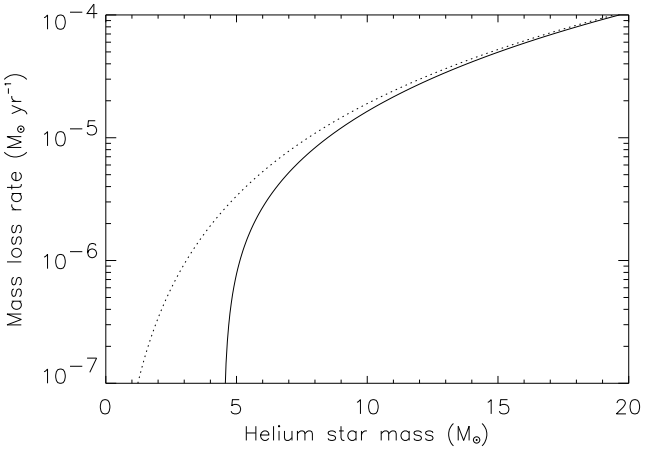

Fig. 2. Stellar wind mass loss rates as a function of helium star mass according to Eqs.(13) and (14) for hydrogenless WN stars (dotted and solid lines, respectively).

He-burning lifetimes and fractions of He-burning spent in WNE and WC/WO substages are taken from Woosley et al. (1993). On the other hand, helium stars revealed by binary interaction when helium is exhausted in the core lose a negligible part of their mass, resulting in pre-supernova He-NS systems with a helium star much more massive than in case B of mass transfer.

The wind-driven secular evolution of He-NS systems is followed according to the Jeans' mode.

2.1.5. Post-helium burning evolution

The advanced evolution of helium stars was first computed by Paczynski (1971) and more recently by Habets (1986b, 1987). In the lower mass range (up to about 3 M$_\odot$), it was found that the outer layers of helium stars evolving at constant mass undergo considerable expansion. Since He-NS systems produced through non-conservative mass transfer phase appear to be very tight, the Roche lobe of low-mass helium stars is reached in almost all of these systems. Furthermore, the outer radii of helium stars between 3 $\sim$ 5 M$_\odot$ show significant expansion so that the mass exchange phase for the closest systems seems unavoidable. Such a mass transfer phase (defined as case BB mass transfer by Delgado & Thomas 1981) can start before or after carbon ignition in the core (cf. Habets 1986a and Avila Reese 1993). In our calculations, a mass exchange sets in if the Roche lobe is smaller than the maximum radius reached at the end of core carbon burning (i.e. point D in the grids of Habets).

Nomoto et al. (1994) proposed that type Ic supernovae such as SN 1994I result from the explosion of bare CO cores that have lost their helium envelope by mass transfer to a close binary companion. It seems unlikely however that CO cores are completely uncovered after mass exchange (Biermann & Kippenhahn 1971, Woosley et al. 1995). As the helium layer is removed, the contribution of the helium burning shell to the luminosity decreases. Once the helium burning shell is extinguished, the star rapidly shrinks and further mass transfer is

avoided. We take arbitrarily an average mass of 0.3 $M_\odot$ for the thin helium layer still covering the CO core. The CO core mass is found from a linear approximation of Habets' evolutionary tracks: $M_{CO} = -0.203 + 0.697\ M_{He}$.

A helium star overflowing its Roche lobe in close He-NS systems, loses its helium envelope in a thermal time-scale. For instance, the corresponding mass transfer rate ranges from 10^{-5} to 10^{-2} $M_\odot\ yr^{-1}$ for a 2.2 $M_\odot$ helium star with an outer radius at the onset of mass transfer ranging from a few solar radii up to red-giant dimensions. As in the first non-conservative mass transfer phase, the outcome of this phase is subject to uncertainties due to the high mass transfer rates involved. Thus, we model this stage with the same spiral-in prescriptions. However, the mass ratio of He-NS systems implies a decrease in orbital separation by about a factor of 2 if nearly all of the helium envelope is ejected in the form of jets from the neutron star (cf. Eq.8). This means that the formation of a CE can be avoided, provided that the above configuration remains stable throughout the entire mass exchange phase. Therefore, we will take values of δ ranging from 0 to 1. The binary is assumed to have merged into a single star if the CO star radius approximated by $R_{CO} = 0.045\ M_{CO}^{0.6}$ does not fit its Roche lobe (Pols & Marinus 1994).

According to Habets (1986b), helium stars more massive than 2.2 $M_\odot$ form an iron core which collapses through photodisintegrations, leaving a neutron star remnant. For helium stars with masses in the range 2.0 to 2.2 $M_\odot$, electron-captures reactions induce a supernova explosion and a neutron star is expected as well. In the following, a helium star less massive than this critical limit is assumed to turn into a O-Ne-Mg white dwarf. An almost bare CO star is expected to undergo a supernova explosion and to leave a neutron star remnant if its CO core mass is larger than the Chandrasekhar mass.

2.2. Results: the formation of pre-supernova binaries

We apply various evolutionary models to initial binaries containing a massive main-sequence star (of mass M_0) and a neutron star companion (of mass 1.35 $M_\odot$) with an orbital separation a_0. Our code follows the evolution of each binary so that we can relate a pre-SN binary system specified by ($M,\ a$) to its progenitor in the ($M_0,\ a_0$) plane. Table 1 gives the parameters used for each model and presents some evolutionary examples. In models A1, A2 and A3, the first Roche lobe overflow directly leads to the formation of a CE whereas a substage of mass ejection through jets from the neutron star is allowed in model B (i.e. 10% of the mass of the hydrogen envelope). Once the helium star overflows its Roche lobe by evolutionary expansion, nearly all the part of the He envelope is transferred to the companion and is ejected through jets in models A1, A2 and B. This second phase of mass transfer is assumed to occur according to the CE scenario in model A3. For each model, a regular grid of 300 x 300 binaries is computed. Fig. 3 shows the regions of formation of pre-SN binary systems. We distinguish four types of pre-SN binary components according to evolutionary paths: CO stars, He stars less massive than 4.5 $M_\odot$, He stars that end up at nearly identical final mass $\sim 5\ M_\odot$ after a stellar wind mass loss phase and finally, He stars revealed by binary interaction when helium is exhausted in the core (independently of their mass).

In all models, the first mass transfer phase produces very close He-NS systems (Table 1), which leads to an important fraction of CO-NS systems among the pre-SN binaries. As expected, major differences appear in evolutionary diagrams if matter is allowed to escape from the system in jets during the first phase, even for a small amount of matter involved (Fig. 3d). A second Roche lobe overflow occurs only in He-NS systems with a low-mass He star. Hence, ejection of the He envelope in the form of jets leads to a small decrease in the orbital separation. If a CE is formed, all He-NS systems may not survive this mass transfer phase (cf. model A3 in Fig. 3c).

Cyg X-3 is a strong X-ray source ($L_x \sim 10^{38}\ erg.s^{-1}$) discovered in 1966 (Giacconi et al. 1967). Observations of strong infrared helium emission lines suggest that this short period X-ray binary (P = 4.79 h) is composed of a compact object and a WR star (Van Kerkwijk et al. 1992). This was already predicted by Van den Heuvel & De Loore (1973) on the basis of evolutionary scenarios. No constraints on the parameters used in our calculations can be derived from this unique observed system at this stage since all models produce easily such short period binaries. Furthermore, according to Lipunov (1992), the propeller effect should impede accretion from the WR-stellar wind onto the neutron star, which is thought to rotate rapidly after the first mass transfer phase. Hence, in view of the high X-ray luminosity of Cyg X-3, Cherepashchuk & Moffat (1994) favor the presence of an accreting black hole, which may explain that Cyg X-3 is the only known X-ray binary containing a WR star.

3. Comparison with observations

The hypothesis of natal kicks imparted to neutron stars during asymmetrical supernova explosion (see e.g. Dewey & Cordes 1987) is supported by recent observations of pulsar's space velocities. In particular, Lyne & Lorimer (1994) found a mean pulsar birth velocity of 450 $\pm$ 90 km/s. In order to find the potential progenitors of the observed binary pulsars (Table 2), the next step will then consist of formulating the post-SN state of the binary relative to the kick velocity and the pre-SN orbital parameters.

3.1. Effects of the kick velocity

Several authors have considered the effect of a random kick velocity on the post-SN orbital characteristics (see e.g. Flannery & Van den Heuvel 1975, Hills 1983, Yamaoka et al. 1993, Brandt & Podsiadlowski 1995, Kalogera 1996). In this section, we will summarize the relationships of interest with regards to this work. Effects of the expanding supernova shell on the companion are ignored since these are thought to be small (Fryxell & Arnett 1981, Yamaoka et al. 1993).

Let us consider a pre-SN binary consisting of a massive star and a neutron star companion with masses M_i and m, moving in a circular orbit with orbital separation a_i. The reference frame is

Table 1. List of the computed evolutionary models. These models are applied to a sample of initial binary systems (M_0, a_0). For each model, the first row gives the new orbital parameters (M_{He}, a) after the non-conservative mass transfer phase; and the second row the new parameters (M_{CO}, a) for binaries that undergo a second stage of mass transfer. All values (M, a) are in solar units.

Models	Input parameters	M_0 10	a_0 300	M_0 11	a_0 1000	M_0 14	a_0 800	M_0 16	a_0 300	M_0 20	a_0 1500	M_0 25	a_0 700
A1	$\delta = 0,\ \alpha_{CE} = 1$	2.53	1.88	3.00	7.19	4.22	4.99	5.11	1.87	7.68	18.3	9.56	4.50
	$\delta = 1$	1.86	1.56	2.19	4.98			3.28	0.75				
A2	$\delta = 0,\ \alpha_{CE} = 0.5$	2.53	0.95	3.00	3.64	4.22	2.52	merger		7.68	9.23	9.56	2.27
	$\delta = 1$	1.86	0.79	2.19	2.52	3.04	1.07						
A3	$\delta = 0,\ \alpha_{CE} = 1$	2.53	1.88	3.00	7.19	4.22	4.99	5.11	1.87	7.68	18.3	9.56	4.50
	$\delta = 0,\ \alpha_{CE} = 1$	1.86	0.25	2.19	0.82			merger					
B	$\delta = 0.1,\ \alpha_{CE} = 1$	2.53	0.92	3.00	3.44	4.22	1.76	merger		7.68	6.68	merger	
	$\delta = 1$	1.86	0.77	2.19	2.38	3.04	0.75						

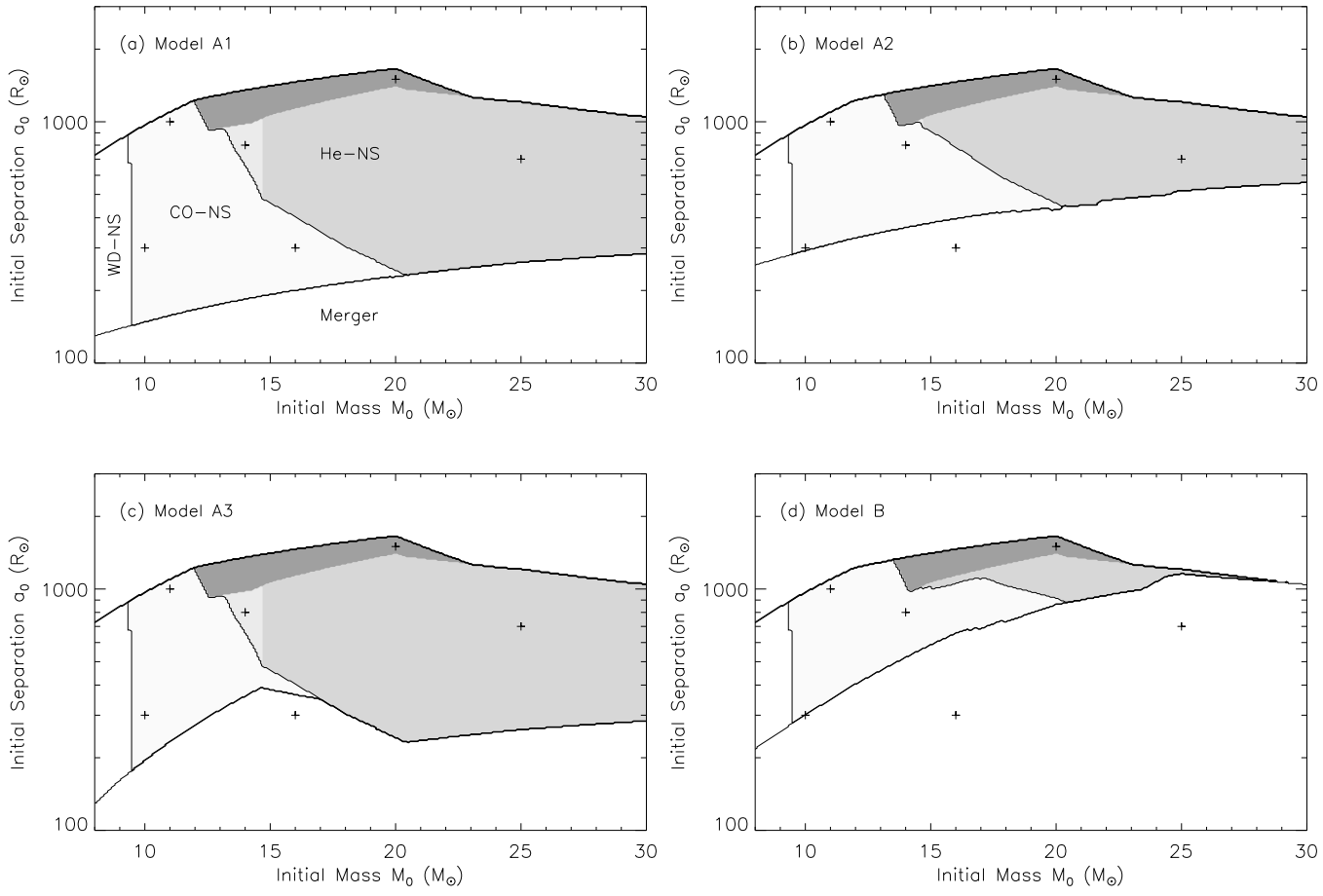

Fig. 3a–d. Evolutionary diagrams of binaries as a function of the initial mass of the massive star M_0 and the initial orbital separation a_0. The pre-supernova binaries consist in He-NS and CO-NS systems. The region of formation of He-NS systems is divided into three parts: the left part (which appears in **a,c** corresponds to He stars less massive than 4.5 $M_\odot$; the right part to He stars that experience a WR-stellar wind mass loss phase and the upper part to He stars stripped of their H-rich envelope after the CHeB stage. The crosses show the location of the binaries listed in table 1.

Table 2. Parameters for the binary pulsars. Errors in the last quoted digits are given in parentheses. Limits on the pre-SN orbital separation a_i are derived according to $a_f(1-e) \leq a_i \leq a_f(1+e)$ (i.e. Eq.20). References: (1) Taylor & Weisberg 1989; (2) Wolszczan 1991; (3) Lyne & Bailes 1990; (4) Nice et al. 1996.

PSR	M_{tot} ($M_\odot$)	M_{psr} ($M_\odot$)	M_c ($M_\odot$)	e	P_{orb} (days)	a_f [a] ($R_\odot$)	a_i ($R_\odot$)	Ref.
B1913+16	2.82837(4)	1.442(3)	1.386(3)	0.617	0.323	2.80	1.07 - 4.53	1
B1534+12	2.679(3)	1.32(3)	1.36(3)	0.274	0.421	3.28	2.38 - 4.18	2
B2303+46	2.9(3)	-	-	0.658	12.34	31.2	10.7 - 51.7	3
J1518+49	2.62(7)	-	-	0.249	8.634	24.6	18.5 - 30.7	4

[a] For PSR B2303+46 and PSR J1518+49, each neutron star mass is assumed to be 1.35 $M_\odot$.

centered on M_i just before the explosion. In this frame, the pre-SN orbital velocity of the massive star relative to its companion chosen to be at rest is given by $V_i = \sqrt{G(M_i+m)/a_i}$. The x-axis corresponds to the line pointing from m to M_i, the y-axis lies along the direction of V_i and the z-axis is perpendicular to the orbital plane. After the explosion, energy conservation allows to express the relative velocity V_f at a distance r as:

$$V_f^2(r) = G(M_f+m)\left(\frac{2}{r} - \frac{1}{a_f}\right) \tag{15}$$

where the subscript f refers to the post-SN state of the binary. Assuming that the instantaneous position r is not changed by the explosion, we can write $\boldsymbol{V_f} = (k_x, V_i + k_y, k_z)$ and $\boldsymbol{r} = (a_i, 0, 0)$ just after the supernova, where $\boldsymbol{k} = (k_x, k_y, k_z)$ is the kick-velocity vector. From energy and angular momentum conservation, this yields:

$$\xi = \left(2 - x\left[\frac{k_x^2 + k_z^2 + (V_i+k_y)^2}{V_i^2}\right]\right)^{-1} \tag{16}$$

$$1 - e^2 = \frac{x}{\xi}\left[\frac{k_z^2 + (V_i+k_y)^2}{V_i^2}\right] \tag{17}$$

$$\cos\theta = \frac{V_i + k_y}{\sqrt{k_z^2 + (V_i+k_y)^2}} \tag{18}$$

where $\xi = a_f/a_i$, x is the ratio of total masses defined as $x = (M_i+m)/(M_f+m)$, e is the eccentricity and θ is the angle between the orbital planes before and after the explosion. From Eqs.(16)-(18), we obtain:

$$\cos\theta = \frac{1}{2}\left[1 - \left(\frac{k}{V_i}\right)^2 + \frac{2\xi - 1}{x\xi}\right]\sqrt{\frac{x}{\xi(1-e^2)}} \tag{19}$$

$$\text{with} \quad (1+e)^{-1} \leq \xi \leq (1-e)^{-1} \tag{20}$$

Since evolutionary models provide the pre-SN parameters (M_i, a_i), the potential progenitors of a peculiar binary pulsar specified by (a_f, e) can be found according to Eq.(20), independently of the kick velocity. Among these potential progenitors, Eq.(19) with the condition $-1 \leq \cos\theta \leq 1$ allows one to find, for a restricted range of the kick, the pre-SN binaries that can produce the required parameters of a specific binary pulsar.

3.2. The formation of binary pulsars

Fig. 4 illustrates the regions of parameter space (M_0, a_0) which allow the formation of the four known binary pulsars. By increasing the kick range velocity, these regions tend to cover all the part of the parameter space corresponding to the potential progenitors as defined above. This is the case for PSR 2303+46, 1534+12 and J1518+49 with kick velocities ranging from 0 to 300 km/s. For PSR 1913+16, the region of potential progenitors is entirely covered for a kick range of 0-500 km/s. Indeed, kick velocities above these limits are allowed but they cannot extend the regions of parameter space any more. Therefore, the more severe constraints on evolutionary models to form a specific binary pulsar come from two necessary conditions independent of the kick: the first one concerning the pre-SN separation a_i is expressed in Eq.(20), i.e. $a_f(1-e) \leq a_i \leq a_f(1+e)$, and the second one requires that the initial orbital separation a_0 is not too large so that binary components can interact.

As an illustration, let us consider the formation of NS-NS systems with large orbital periods like PSR 2303+46 and PSR J1518+49. From Fig. 4, one can easily see that the extent of the progenitors region is extremely sensitive to the spiral-in prescriptions. Actually, the case of PSR J1518+49 is the most interesting because of its moderate eccentricity. As a consequence, the minimum pre-SN orbital separation is 18.5 $R_\odot$, whereas the corresponding value is 10.7 $R_\odot$ for PSR 2303+46 (cf. Table 2). The huge orbital shrinkage in models A2 and B can never lead to such a large value of a_i. Therefore, under the assumption that the same evolutionary picture holds for the four binary pulsars, the newly discovered system PSR J1518+49 favors a full CE-evolution with α_{CE} close to unity according to the formalism used for the mass transfer phase.

In all models, the pre-SN binaries of these two binary pulsars consist of He-NS systems which are formed through a case C mass transfer. On the contrary, PSR 1913+16 and PSR 1534+12 are likely to have experienced a case B mass transfer. In model A1, evolutionary expansion of the He star progenitor may lead to a second mass exchange phase. Since ejection of matter in the form of jets induces a small decrease in the separation, PSR 1913+16 and PSR 1534+12 may be the product of a type Ic supernovae in a CO-NS system. This feature seems very prob-

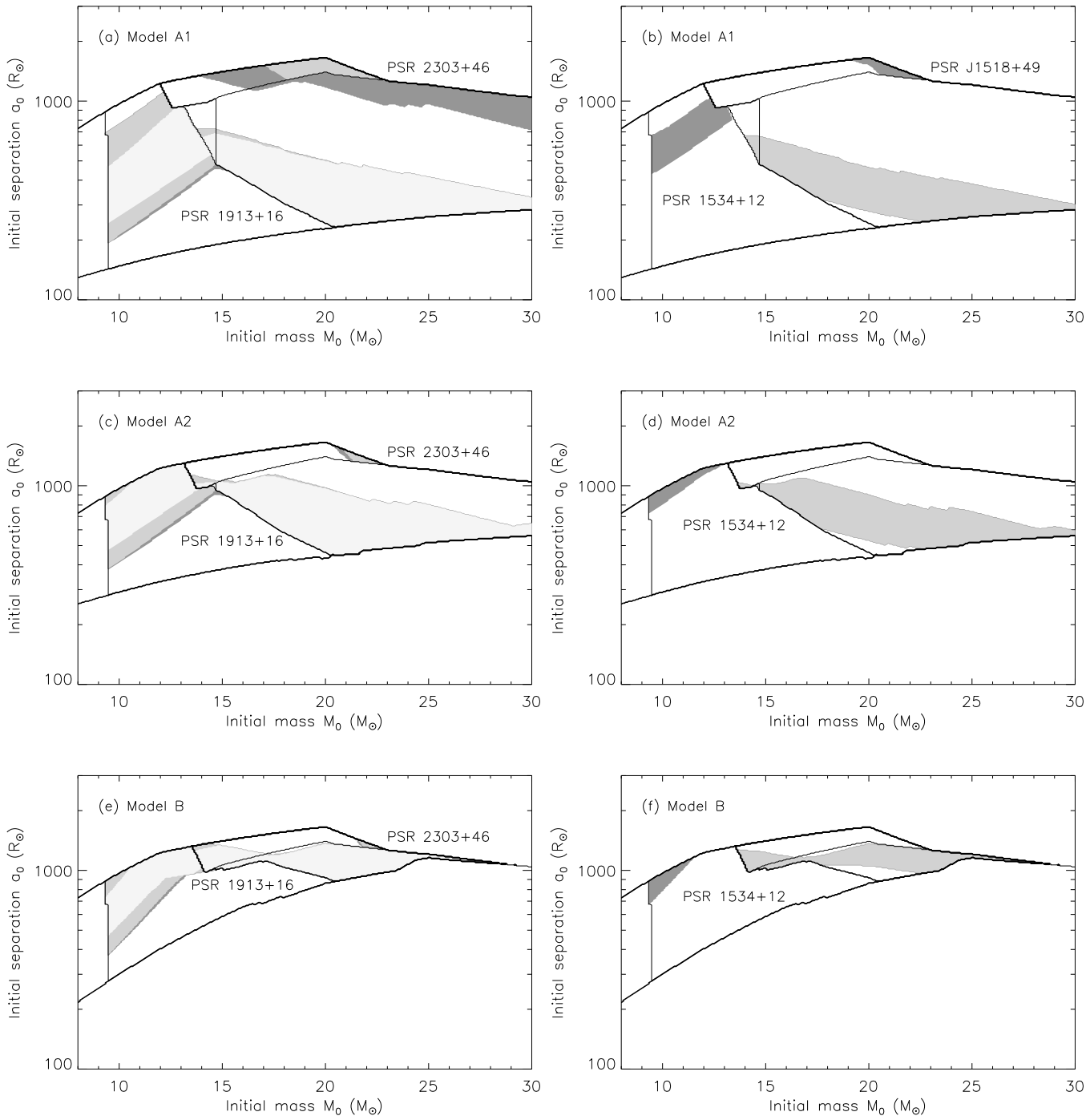

Fig. 4a–f. Regions of the potential progenitors systems of the four known binary pulsars in the (M_0, a_0) plane. The dark shaded region is related to the progenitors of a specific NS-NS system in the case of a kick velocity less than 150 km/s. The medium shaded area corresponds to the extension of the previous region when the kick velocity ranges from 0 to 300 km/s. According to Eq.(20), other potential progenitors may exist in the (M_0, a_0) plane, i.e. in the case of higher kicks. These systems are represented by the light shaded region (i.e. case of PSR 1913+16). Different types of pre-SN binaries are delimited by solid lines (cf. Fig. 3). Model A3, which is not represented, is similar to model A1, except that pre-SN progenitors of binary pulsars do not contain CO stars. In models A2 and B, potential progenitors cannot be found for PSR J1518+49.

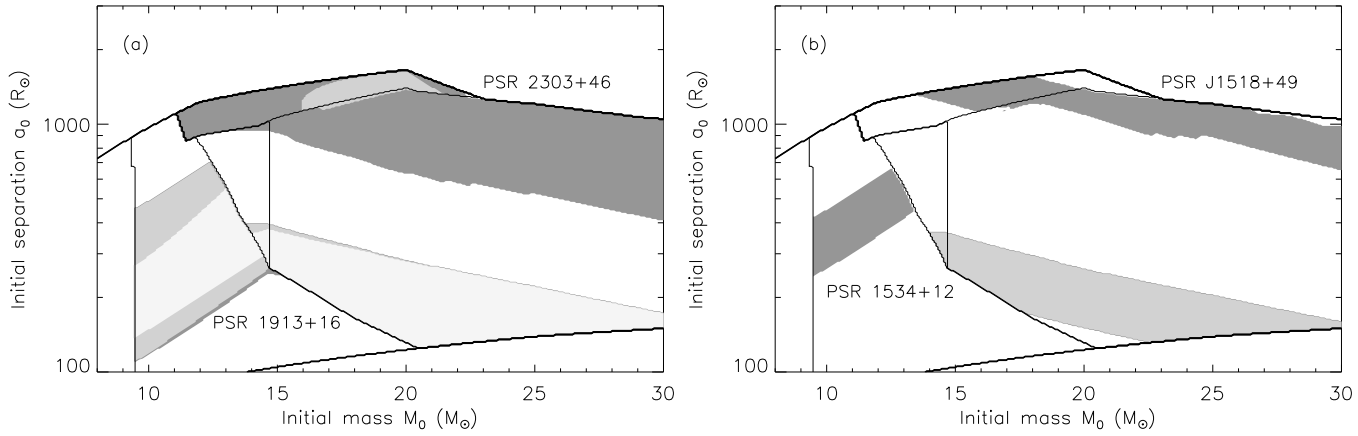

Fig. 5a and b. Regions of the progenitors systems of the four known binary pulsars in the (M_0, a_0) plane. In this model, the first mass transfer phase involves the formation of a CE as soon as the neutron star comes into contact with the evolved star. The efficiency parameter is α_{CE} = 0.5, see Sect. 4.2 for the formalism used for CE-evolution. During the second stage of mass transfer, the excess overflowing matter is thought to be ejected in the form of jets from the neutron star. The gray-scale code is the same as in Fig. 4.

able in the case of low kicks for PSR 1534+12 (i.e., $\leq$ 150 km/s) or moderate kicks for PSR 1913+16 (i.e., $\leq$300 km/s). On the other hand, the high mass transfer rate involved in the second mass exchange phase may lead to the formation of a CE (model A3). In this case, the orbit of remnant CO-NS systems is too close to produce the required parameters. Following this scenario, PSR 1913+16 and PSR 1534+12 are the product of a type Ib supernovae in a He-NS system.

4. Discussion

4.1. Evolution of accretion stars

The massive star may have previously accreted matter from the progenitor of the neutron star. In this paper, the main-sequence star evolves as a single star until it first fills its Roche lobe, according to the works of Hellings (1983) and Vanbeveren (1990) who showed that the further evolution of accretion stars is almost identical to the evolution of a corresponding single star. However, while considering the effect of molecular weight gradients on convection, Braun & Langer (1995) found that this rejuvenation process of the mass gaining star does not always take place, but appears to depend mainly on the rate of mixing in the semiconvective layer which forms above the convective core upon accretion. The main result of a non-rejuvenation is an internal chemical structure which is quite unlike that occurring in any single star, leading to a different track in the HR diagram. According to Braun & Langer, a non-rejuvenated star spends its whole post main-sequence evolution as a blue supergiant whereas the corresponding massive single star evolves into a red supergiant.

This feature may have important consequences on the outcome of high-mass binary evolution. Taking the characteristic values of a blue supergiant (e.g. $\log T_{eff} \sim 4.1,\ \log L/L_\odot \sim 5.1$), one finds that evolutionary expansion of a non-rejuvenated star will lead to a spiral-in of the neutron star companion if the orbital separation is less than $\sim$ 150 $R_\odot$. Such a configuration implies that very few systems can survive the mass transfer phase. Furthermore, binary pulsars with large orbital periods like PSR J1518+49 cannot be formed in this way. Among other basic parameters, Braun & Langer showed that rejuvenation is more likely for accreting stars of initial moderate mass. For instance, according to their model #5, a 12 $M_\odot$ which accretes 8 $M_\odot$ adopts a chemical structure comparable to a 20 $M_\odot$ single star, whereas a 20 $M_\odot$ (model #12) does not perform rejuvenation for the same amount of accreted matter. Therefore, we expect little changes at least for the left part of the evolutionary diagrams computed in this paper (i.e., $M_0 \leq 20\ M_\odot$). However, Braun & Langer pointed out that none of their models lead to rejuvenation if a low value is adopted for the efficiency parameter of semiconvection. In such a case, the merger rate of NS-NS systems would be considerably smaller than expected.

4.2. The formation of PSR 2303+46 and PSR J1518+49

In Sect. 3.2, it was shown that the formation of binary pulsars with large orbital periods requires a moderate orbital shrinkage during the preceding mass transfer phase. This can be accomodated if one adopts a full CE-evolution with $\alpha_{CE} \sim 1$. However, using the same formalism for CE-evolution, Van den Heuvel et al. (1994) argue that a progenitor cannot be found for PSR 2303+46. This result was established in the case of a symmetric supernova explosion, for which the smallest possible pre-SN separation is obtained, namely $a_i = a_f(1-e)$. If a kick is imparted to the neutron star, the pre-SN separation is larger, which seems a less favourable configuration. Actually, we do not find any progenitors for PSR 2303+46 nor for PSR J1518+49 in the spherically symmetric case. For instance, from the parameters of PSR 2303+46, we derive a helium star of 3.13 $M_\odot$ at the time of explosion, which corresponds to a 11.5 $M_\odot$ initial companion mass. Equation (3) then yields a pre-spiral-in separation 165 times larger than that of the post-spiral-in system, whereas Van den Heuvel et al. found a value of 235. This

departure comes from the different assumptions we have used for the neutron star mass, the normalized Roche lobe radius r_L (Eq.1) and the relationship between the helium core and the hydrogen star masses (Eq.10). Nevertheless, both values lead to a pre-spiral-in separation much too large to allow a mass transfer event.

On the other hand, a binary can survive an asymmetric supernova explosion even if the amount of mass ejected is high enough to disrupt the system in the symmetric case. So, let us consider a binary containing a 20 $M_\odot$ initial hydrogen star with an orbital separation of 1500 $R_\odot$ (cf. system #5 in Table 1). Due to the large separation, the massive star overflows its Roche lobe in the late burning phases. As a result of the time spent on the RSG branch, the stellar mass has dropped to 16.6 $M_\odot$ while the separation has slowly increased up to 1790 $R_\odot$ at the onset of mass transfer. The CE-evolution then gives a 7.68 $M_\odot$ helium star with a separation of 18.3 $R_\odot$, i.e. an orbital shrinkage factor of 98. Therefore, a stage of heavy mass loss by stellar wind prior to spiral-in leads to a moderate orbital shrinkage and hence, favors the formation of binary pulsars with large orbital periods.

From their results, Van den Heuvel et al. (1994) propose an alternative evolutionary picture for the formation of PSR 2303+46. In this model, a very massive star ($\geq$40-45 $M_\odot$) spontaneously sheds its hydrogen-rich envelope during a LBV phase, without transferring mass to the neutron star companion (see also Kaper et al. 1995). Then, a decrease of the orbital separation may result from the frictional torque acting on the neutron star immersed in the dense wind. Nice et al. (1996) point out that the same scenario may also explain the wide orbit of the newly discovered binary pulsar PSR J1518+49.

The restricted region of potential progenitors (Fig. 4b) may suggest that PSR J1518+49 is unlikely to be formed through standard evolutionary models. However, the high sensitivity of the outcome of the mass transfer phase to the spiral-in prescriptions implies that the inverse problem (i.e. the finding of progenitors) is not robust. In addition, the efficiency parameter α_{CE} may be formally larger than unity if additional energy sources other than orbital energy contribute to mass ejection, such as accretion energy or recombination energy in ionization zones (see e.g. the review of Iben & Livio 1993 for other possible processes).

Furthermore, we have considered so far the formalism for CE-evolution according to Eq.(3), which is the most commonly used in the Monte-Carlo simulations. In principle, these simulations can limit the possible range of α_{CE} by trying to reproduce the parameters of well-studied binaries (e.g. De Kool 1990). Another approach in literature consists of performing hydrodynamical calculations that can follow the dynamical phase of CE-evolution (Livio & Soker 1988; Taam & Bodenheimer 1989, 1991; Terman et al. 1995 and references therein). These numerical computations start from an initial configuration consisting of the two cores surrounded by an envelope of diameter $\sim 2a_i$ and lead to small values of α_{CE} in the range $\sim$ 0.3-0.6. These works attempt to quantify the CE-phase according to the following expression:

$$\frac{G(M_i + m)(M_i - M_f)}{2a_i} = \alpha_{CE}\frac{GM_f m}{2}\left(\frac{1}{a_f} - \frac{1}{a_i}\right) \qquad (21)$$

It is important to realize that differences between these two formalisms (i.e. Eqs. 2,21), and hence between the values of α_{CE}, reflect the difficulty in estimating the binding energy of the envelope at early and late times at the CE-phase (Rasio & Livio 1996).

As a last model, we perform evolutionary calculations according to this formalism. When the massive star begins overflowing its Roche lobe, we assume that some drag force brings the two stars into contact during the early dynamical phase, so that the new separation a_i corresponds to the stellar radius of the primary (cf. Terman et al. 1994). Then, we apply Eq.(21) for the phase of strong dynamical interaction with an efficiency parameter α_{CE} of 0.5 (cf. Fig. 5). Such an initial configuration for CE-evolution may also appear after a substage of fast mass transfer in the form of jets (see Sect. 2.1.3) or as a consequence of the Darwin instability. In this model, the configuration just prior the spiralling-in process for the 20 $M_\odot$+1.35 $M_\odot$ system#5 consists of a 16.6 $M_\odot$+1.35 $M_\odot$ binary with an orbital separation of 1060 $R_\odot$. Then, the system achieves a post-spiral-in separation of 33.2 $R_\odot$. We emphasize that the assumption of a pre-spiral-in separation a_i equal to the separation at the onset of mass transfer (e.g. 1790 $R_\odot$ in system #5) would lead to an even more favourable situation for the formation of binary pulsars (cf. Tutukov & Yungelson 1993, 1994).

Therefore, from Figs. 4-5, we conclude that it is well conceivable that binary pulsars with a wide orbit may have been formed through standard evolutionary models involving a CE-event. In particular, this picture holds for PSR J1518+49 provided that CE-evolution leads to a moderate orbital shrinkage.

Acknowledgements. I am grateful to G. Le Denmat for initiating this study and to N. Langer and E.P.J. Van den Heuvel for their comments on the manuscript.

References

Avila Reese V.A., 1993, Rev. Mexicana Astron. Astrof. 25, 79
Bagot P., 1996, A&A 314, 576
Bailes M., 1996, in "Compact stars in binaries", Eds Van Paradijs J.A., Van den Heuvel E.P.J., Kuulkers E., (Kluwer, Dordrecht), p.213
Bhattacharya D., Van den Heuvel E.P.J., 1991, Physics Rep, 203, 1
Biermann P., Kippenhahn R., 1971, A&A 14, 32
Brandt N., Podsiadlowski P., 1995, MNRAS 274, 461
Braun H., Langer N., 1995, A&A 297, 483
Brown G.E., 1995, ApJ 440, 270
Cherepashchuck A.M., 1981, MNRAS 194, 761
Cherepashchuck A.M., Moffat A.F.J., 1994, ApJ 424, L53
Chernoff D.F., Finn L.S., 1993, ApJL 411, L5
Chevalier R.A., 1993, ApJ 411, L33
Chevalier R.A., 1996, ApJ 459, 322
Clark J.P.A., Van den Heuvel E.P.J., Sutantyo W., 1979, A&A 72, 120
Counselman C.C., 1973, ApJ 180, 307
Crampton D., Cowley A.P., Hutchings J.B., 1980, ApJ 235, L131

Curran S.J., Lorimer D.R., 1995, MNRAS 276, 347
De Kool M., 1990, ApJ 358, 189
Delgado A.J., Thomas H.C., 1981, A&A 96, 142
De Loore C.W.H., Vanbeveren D., 1994, A&A 292, 463
Dewey R.J., Cordes J.M., 1987, ApJ 321, 780
Eggleton P.P., 1983, ApJ 268, 368
Flannery B.P., Van den Heuvel E.P.J., 1975, A&A 39, 61
Fryxell B.A., Arnett W.D., 1981, ApJ 243, 994
Giacconi R., Gorenstein P., Gursky H., Waters J.R., 1967, ApJ 148, L119
Glatzel W., Kiriakidis M., Fricke K.J., 1993, MNRAS 262, L7
Habets G.M.H.J., 1986a, A&A 165, 95
Habets G.M.H.J., 1986b, A&A 167, 61
Habets G.M.H.J., 1987, A&AS 69, 183
Hellings P., 1983, Ap&SS 96, 37
Hills J.G., 1983, ApJ 267, 322
Hjellming M.S., Webbink R.F., 1987, ApJ 318, 794
Iben I.Jr., Livio M., 1993, PASP 105, 1373
Kalogera V., 1996, preprint
Kaper L., Lamers J.J.G.L.M., Ruymaekers E., Van den Heuvel E.P.J., Zuiderwijk E.J., 1995, A&A 300, 446
Kippenhahn R.,Weigert A., 1967, ZA 65, 251
Kiriakidis M., Fricke K.J., Glatzel W., 1993, MNRAS 264, 50
Kornilov V.G., Lipunov V.M., 1983a, AZh 60, 284
Kornilov V.G., Lipunov V.M., 1983b, AZh 60, 574
Langer N., 1989a, A&A 210, 93
Langer N., 1989b, A&A 220, 135
Langer N., 1994 in "Wolf-Rayet stars: binaries, colliding winds, evolution", Kluwer (IAU-symposium 163), Eds. Van der Hucht K.A. & Williams P.P.
Langer N., Hamann W.R., Lennon M., Najarro F., Pauldrach A.W.A., Puls J., 1994, A&A 290, 819
Lipunov V.M., 1992, "Astrophysics of Neutron stars", Springer Verlag, Heidelberg
Lipunov V.M., Postnov K.A., Prokhorov M.E., 1996, A&A 310, 489
Livio M., Soker N., 1988, ApJ 329, 764
Lyne A.G., Bailes M., 1990, MNRAS 246, 15p
Lyne A.G., Lorimer D.R., 1994, Nature 369, 127
Margon B., 1984, Ann. Rev. Astron. Astrophys. 22, 507
Meurs E.J.A., Van den Heuvel E.P.J., 1989, A&A 226, 88
Narayan R., Piran T., Schemi A., 1991, ApJ 379, L17
Nice D.J., Sayer R.W., Taylor J.H., 1996, ApJL in press
Nomoto K., Yamaoka H., Pols O.R., Van den Heuvel E.P.J., Iwamoto K., Kumagai S., Shigeyama T., 1994, Nature 371, 227
Paczynski B., 1971, Acta Astron. 21, 1
Phinney E.S., 1991, ApJ 380, L17
Pols O.R., Marinus M., 1994, A&A 288, 475
Portegies Zwart S.F., Spreeuw H.N., 1996, A&A 312, 670
Portegies Zwart S.F., Verbunt F., 1996, A&A 309, 179
Rasio F.A., Livio M., 1996, preprint
Rathnasree N., 1993, MNRAS 260, 717
Schaller G., Schaerer D., Meynet G., Maeder A., 1992, A&AS 96, 269
Schutz B.F., 1986, Nature 323, 310
Shakura N.I., Sunyaev R.A., 1973, A&A 24, 337
Shore S.N., Livio M., Van den Heuvel E.P.J. 1994 in Nussbaumer H., Orr S. (eds), "Binaries as tracers of stellar evolution", Springer Verlag, Berlin Heidelberg p.263
Taam R.E., Bodenheimer P., 1989, ApJ 337, 849
Taam R.E., Bodenheimer P., 1991, ApJ 373, 246
Taylor J.H., Weisberg J.M., 1989, ApJ 345, 434
Terman J.L., Taam R.E., Hernquist L., 1994, ApJ 422, 729
Terman J.L., Taam R.E., Hernquist L., 1995, ApJ 445, 367
Thorsett S.E., Arzoumanian Z., Mc Kinnon M.M., Taylor J.H., 1993, ApJ 405, L29
Tutukov A.V., Yungelson L.R., 1993, MNRAS 260, 675
Tutukov A.V., Yungelson L.R., 1994, MNRAS 268, 871
Vanbeveren D., De Greve J.P., 1979, A&A 77, 295
Vanbeveren D., 1990, A&A 234, 243
Van den Heuvel E.P.J., De Loore C., 1973 , A&A 25, 387
Van den Heuvel E.P.J., Lorimer D.R., 1996, MNRAS 283, L37
Van den Heuvel E.P.J., Ostriker J.P., Petterson J.A., 1980, A&A 81, L7
Van den Heuvel E.P.J., Kaper L., Ruymaekers E., 1994 in "New horizon of X-ray Astronomy", eds. F. Makino & T. Ohashi, Tokyo: Universal Academy Press, p.75
Van Kerkwijk M.H., Charles P.A., Geballe T.R., King D.L., Miley G.K., Molnar L.A., Van den Heuvel E.P.J., Van der Klis M., Van Paradijs J., 1992 , Nature 355, 703
Webbink R.F., 1984, ApJ 277, 355
Verbunt F., Van den Heuvel E.P.J., 1995 in "X-ray binaries", eds Lewin W.H.G., Van Paradijs J., Van den Heuvel E.P.J., Cambridge University Press, p.457
Wolszczan A., 1991, Nature 271, 38
Woosley S.E., Langer N., Weaver T.A., 1993, ApJ 411, 823
Woosley S.E., Langer N., Weaver T.A., 1995, ApJ 448, 315
Yamaoka H., Shigeyama T., Nomoto T., 1993, A&A 267, 433
Zahn J.-P., 1977, A&A 57, 383
Zealey W.J., Dopita M.A., Malin D.F., 1980, MNRAS 192, 731

This article was processed by the author using Springer-Verlag LaTeX A&A style file *L-AA* version 3.